A Fully Coupled Computational Model of the Silylation Process

W. Winters*, G. Evans**, V. Prantil*** and R. Larson****

*Sandia National Laboratories, Livermore, CA, USA, winters@sandia.gov
**Sandia National Laboratories, Livermore, CA, USA, evans@sandia.gov
***Milwaukee School of Engineering, Milwaukee, WI, USA, prantil@msoe.edu
****Sandia National Laboratories, Livermore, CA, USA, rslarso@sandia.gov

ABSTRACT

This paper describes a fully coupled computational model of the positive tone silylation process. The model is two-dimensional and transient and focuses on the part of the lithography process in which crosslinked and uncrosslinked resist is exposed to a gaseous silylation agent. The model accounts for the combined effects of mass transport, chemical reaction, the generation of stresses, and the resulting material motion. The influence of stress on diffusion and reaction rates is also included. Both Fickian and case II diffusion models have been incorporated. A complete 2D transient simulation of the silylation process is presented and discussed.

Keywords: EUVL, TSI, FEM, diffusion, silylation,

1 INTRODUCTION

Top surface imaging (TSI) based on silylation has shown promise for high resolution/high aspect ratio imaging in 193 nm and EUVL applications. Achieving the required 2-4 nm line edge roughness continues to be a significant research and development challenge for future TSI systems, however. The present work was undertaken to better understand the complex phenomena related to the silylation step in TSI. The model discussed here accounts for multispecies diffusion of the silylation and product gases, the silylation chemical reaction, the subsequent swelling and movement of the resist and adjacent materials, and the evolution of the stress state including the kinematics for finite deformation. Material properties and constants were estimated from the literature.

Pierrat [1] developed an early model of the silylation process. His work was extended by Zuniga and Neureuther [2] to include stress. The model presented here can be considered an extension of their work.

2 PROBLEM DESCRIPTION

The TSI processing steps are described in detail in references [3,4]. Only the silylation step will be described here. The purpose of the silylation step is to increase the silicon content in the uncrosslinked (unexposed) areas of the resist, thereby increasing etch selectivity for subsequent processing steps. The top surface of the imaging layer is exposed to a gaseous aminodisilane. This silylation agent diffuses preferentially through the uncrosslinked regions where a localized chemical reaction occurs, causing silicon uptake, an increase in volume, and liberation of a product gas. The magnitude and shape of the volume expansion depends on the reaction/diffusion process and the resulting stress state in the material. Figure 1 shows a cross-sectional plasma stain of a silylated sample. Exposure results in a series of parallel crosslinked regions that run perpendicular to the cross-section cut. The expanded silylated sections appear light colored. Predicting the size and shape of the volume expansions is the primary motivation behind developing the present model. The sample also shows a small degree of silylation (typically less than 20 nm) in the exposed areas. Such unwanted silylation is often referred to as the "scum layer" and is believed to occur because of acid loss during a previous post exposure bake step [3,4]

3 MODEL FORMULATION

3.1 Mass Transfer and Chemistry

Following Pierrat's [1] mechanism, silylating agent, A, is assumed to react with the unsilylated resist, C, releasing amines, B, and forming silylated but unexpanded resist, D, which subsequently swells to the expanded resist, E:

$$A + C \xrightarrow{k_s} B + D \tag{1}$$

$$D \xrightarrow{k_e} E \tag{2}$$

Species A and B are transported within the resist by diffusion. The material model requires that the mass transfer process be described relative to the material motion (Lagrangian formulation). A control volume finite element discretization (Schneider [5]) is used in which resist material species C, D, and E do not cross control volume boundaries. The time rate of change of mass of species A in a control volume is given by:

$$\frac{dm_A}{dt} = \dot{\omega}_A V - \int_S \left[\mathbf{j}_A + \frac{\tilde{\rho}_A \varepsilon_A (\mathbf{j}_A + \mathbf{j}_B)}{\tilde{\rho}_C \varepsilon_C + \tilde{\rho}_D \varepsilon_D + \tilde{\rho}_E \varepsilon_E} \right] \bullet \mathbf{n} dS \tag{3}$$

where $\dot{\omega}$, $\tilde{\rho}$, ε, and $\mathbf{j}$ are the volumetric mass production rate, intrinsic density, volume fraction, and mass diffusion flux respectively. V and S are the volume and surface area

of the control volume, respectively. Similar equations describe mass conservation of the other species except that equations for species C, D, and E do not contain the surface integral term, since for those species mass is not allowed to cross the control volume boundary. For constant intrinsic density and volume fractions that sum to unity, the species mass conservation equations can be added together to yield a relation for the unconstrained volumetric expansion rate:

$$\dot{V} = \sum_k \frac{\dot{\omega}_k}{\tilde{\rho}_k} V - \oint_S \left[\frac{\mathbf{j}_A}{\tilde{\rho}_A} + \frac{\mathbf{j}_B}{\tilde{\rho}_B} + \frac{(\varepsilon_A + \varepsilon_B)}{(\tilde{\rho}_C \varepsilon_C + \tilde{\rho}_D \varepsilon_D + \tilde{\rho}_E \varepsilon_E)} (\mathbf{j}_A + \mathbf{j}_B) \right] \bullet \mathbf{n} dS \quad (4)$$

The mass consumption rate of species A is:

$$\dot{\omega}_A = -k_s \rho_A \rho_C / M_C \quad (5)$$

where k_s is the rate constant for the silylation reaction, ρ_A and ρ_C are the mass concentrations of species A and C, respectively, and M_C is the molecular weight of species C. Analogous expressions hold for the production and consumption rates of other species. Mass diffusion fluxes of species A and B relative to the mass average velocity are:

$$\mathbf{j}_{A,B} = -\rho D_o \exp(w \rho_E / M_E) \nabla (m_{A,B} / m) \quad (6)$$

where the exponential is used to describe non-Fickian diffusion in polymers (Crank [8]) and m is mixture mass. The model allows for either Dirichlet or flux boundary conditions at the gas/polymer interface for the two diffusing species A and B. For Dirichlet conditions, concentrations are specified at the boundary; for flux conditions the following is used

$$\dot{m}_{A_g} = K_g \left(p_{A_{g,\infty}} - H Y_{A_{r,s}} M_{\text{mixture}_{r,s}} / M_A \right) \quad (7)$$

where $\dot{m}_{A_g}$ is the specified mass flux of A from the gas into the surface, $p_{A_{g,\infty}}$ is the partial pressure of A far from the interface, H is Henry's constant, and $Y_{A_{r,s}}$ is the mass fraction of A in the resist at the surface; the concentration of product species B is set to zero at the boundary.

3.2 Momentum

The material motion is obtained from the conservation of momentum, *i.e.*

$$\partial(\rho \mathbf{v}) \partial t = \nabla \bullet \sigma \quad (8)$$

where $\rho, \mathbf{v},$ and σ are the density, velocity vector, and stress tensor, respectively. Although the material motion is quasi-steady, a portion of the transient term is retained to facilitate integration in time along with the mass transport equations. Hence the momentum equation reduces to

$$\rho \dot{\mathbf{v}} = \nabla \bullet \sigma \quad (9)$$

3.3 Polymer Material Response

The polymer constitutive model is based on the glassy inelastic flow model of Boyce, Parks and Argon [8]. Resistance to deformation arises from two physical mechanisms: polymer chain rotation and the decrease in entropy accompanying the resulting ordered state. The polymer stress evolves with an objective rate given by:

$$\dot{\sigma} - W\sigma - \sigma W = [2\mu II + \lambda I \otimes I] : \left(D - D^p - \left\{ \alpha \dot{\theta} + \frac{\dot{\mathrm{V}}}{\mathrm{V}} \right\} I \right) \quad (10)$$

where D and W are the symmetric and skew parts of the velocity gradient, respectively, θ is the absolute temperature, α is the coefficient of thermal expansion, and μ, λ are the elastic constants. The inelastic part of the deformation rate tensor is prescribed by an associative flow law

$$D^p = \dot{\gamma}_0 \exp\left[\frac{-As}{\theta} \left\{ 1 - \frac{\tau}{s} \right\}^{\frac{p}{q}} \right] \frac{\sigma' - \beta}{|\sigma' - \beta|} \quad (11)$$

where s is the flow resistance associated with chain rotation, β is a back-stress tensor representing internal resistance to highly ordered chain alignment, and $\dot{\gamma}_0, A, p, q$ are constants determined by material tests [4,8]. The back-stress remains coaxial with the left plastic stretch tensor with principal values given by:

$$\beta_i = C^R \frac{\sqrt{N}}{3} \left[V_i^p \aleph^{-1}\left(\frac{V_i^p}{\sqrt{N}} \right) - \frac{1}{3} \sum_{j=1}^{3} V_j^p \aleph^{-1}\left(\frac{V_j^p}{\sqrt{N}} \right) \right] \quad (12)$$

where the plastic deformation gradient is

$$F^p = V^p R, \quad (13)$$

C^R is the rubbery modulus and the Langevin function is given by:

$$\aleph(\eta_i) = \coth(\eta_i) - \frac{1}{\eta_i} = \frac{V^p}{\sqrt{N}} \quad (14)$$

This back-stress is analogous to a nonlinear spring that acts in parallel to a softening viscous dashpot representing the resistance to polymer chain rotation. For strains of up to 30%, the viscous flow resistance exhibits a softening upon yield, the so-called yield drop. For strains approaching 100%, the decrease in entropy accompanying alignment of long-chained polymer molecules dominates the flow resistance, leading to a locking behavior where deformation becomes limited as the polymer stress increases.

4 SOLUTION METHOD

The finite element method is used to solve the coupled silylation equations. Details of the procedure are presented in [6]. Only a general overview will be presented here.

The computational space is discretized into four node quad elements. Application of the control volume finite element method for mass transport and Galerkin's method for motion yields a set of ordinary differential equations in time for the nodal variables (x and y velocity components and the nodal masses of species *A*, *B*, *C*, *D*, and *E*). Bilinear shape functions are used for spatial integration. Four-point quadrature is used to integrate the mass transport equations. In the equation of motion the components of the stress tensor are integrated in time at one element gauss point. At the expense of a small time step restriction (necessary for implementation and only for the solution of material point stress), a quasi-yield function was defined, making solution of the stress evolution by a radial return algorithm possible and generally more robust than a coupled Newton-Raphson solution. Time integration is performed explicitly and density scaling is used to integrate the momentum equation so that a larger time step can be used. This scaling has no influence on the solution since inertia terms remain small.

5 RESULTS

The example calculation here models a process similar to that shown in Figure 1. Figure 2 shows the computational mesh. A resist $4x10^{-5}$ cm in thickness is bonded to a rigid surface. Part of the free surface has been crosslinked to a depth of $6x10^{-6}$ cm. The planes of symmetry simulate a series of silylation lines parallel to the z-axis. The distance between any two adjacent silylation centerlines is $4.8x10^{-5}$ cm. Crosslinked behavior is modeled by reducing the diffusivity of the silylation agent in crosslinked elements by three orders of magnitude. The properties used were estimated from the literature and are summarized in [4].

Initially the resist is assumed to be unsilylated; *i.e.* it is composed entirely of species *C*. At time zero the free surface is exposed to the silylation agent, species *A*, and mass transport, chemistry and material swelling proceed for a simulated time of 60 seconds.

Boundary conditions for the problem are summarized as follows: The volume fractions of species *A* and *E* at the surface are assumed to be .05 and .95 respectively. Mass transfer does not occur at the bottom or symmetry surfaces. The upper surface is stress free. Symmetry surfaces permit only y direction movement and the lower surface is fixed.

Figure 3 shows cross-sections of silylation agent concentration and material swelling for 0, 1, 3, 5, 10, 30 and 60 seconds. To aid in visualization, results have been mirrored across the left symmetry plane. The silylation agent diffuses preferentially into the uncrosslinked resist causing swelling similar to that observed in Figure 1. Because of reduced diffusivity in the crosslinked region, mass transport, chemistry and swelling are localized to a thin layer along the free surface. This layer is most visible at t=60 seconds and resembles the so-called "scum" layer observed after actual silylation experiments.

Figure 4 shows contours of shear stress at t=60 seconds. The polymer material model predicts that significant inelastic deformation occurs in this time frame. This flow is driven predominantly by the volumetric swelling rates characteristic of the silylation process. In such cases, the volume-conserving nature of plastic flow dictates that the amount of swelling can, at best, be only marginally affected by the stress state. This kinematic constraint, *i.e.* the geometry of the crosslinked region, however, can play a significant role in the overall shape change of the material. The relationship between crosslinked and uncrosslinked regions at the conclusion of the simulation is shown in Figure 5. Elements in the crosslinked region are colored darker relative to the elements in the uncrosslinked region. As expected, nearly all material swelling has been confined to the uncrosslinked region. Some swelling is evident in the crosslinked area along the free surface ("scum layer") and in the interior interface between the crosslinked and uncrosslinked regions. This was to be expected since the crosslinked region was assigned a finite (but relatively low) diffusion coefficient and the silylation reaction was permitted to proceed unimpeded when the silylation agent was present. In this simulation, silylation extends to the material below the crosslinked region. The resulting swelling causes upward movement of the crosslinked material. Such movement is likely to occur when crosslinking is shallow and silylation times are long.

Acknowledgment: Funding was provided by the Extreme Ultraviolet Limited Liability Company under a Cooperative Research and Development Agreement and Sandia/US DOE contract DE-AC04-94AL85000.

REFERENCES

[1] C. Pierrat, J. Vac. Sci. Technol. B 10(6), 2581, 1992.

[2] M. Zuniga and A. R. Neureuther, J. Vac. Sci. Technol. B 14,(6),4221,1996

[3] C. Henderson, D. Wheeler, T. Pollagi, G. Cardinale, D. O'Connell, A. Fisher and J. Goldsmith, Emerging Lithographic Technologies II Proc. SPIE 3331,1998.

[4] W. Winters, G. Evans, R. Larson, and V. Prantil, SAND99-8225, 1999.

[5] G. Schneider, Handbook of Numerical Heat Transfer, pp. 379-420, ed. Minkowycz, Sparrow, Schneider, and Pletcher, Wiley & Sons, New York, 1988.

[6] J. Crank, The Mathematics of Diffusion, 2nd ed., Clarendon Press, Oxford, 1975

[7] M. C. Boyce, D.M. Parks, and A. S. Argon, Mechanics of Materials, 7, 115,1988

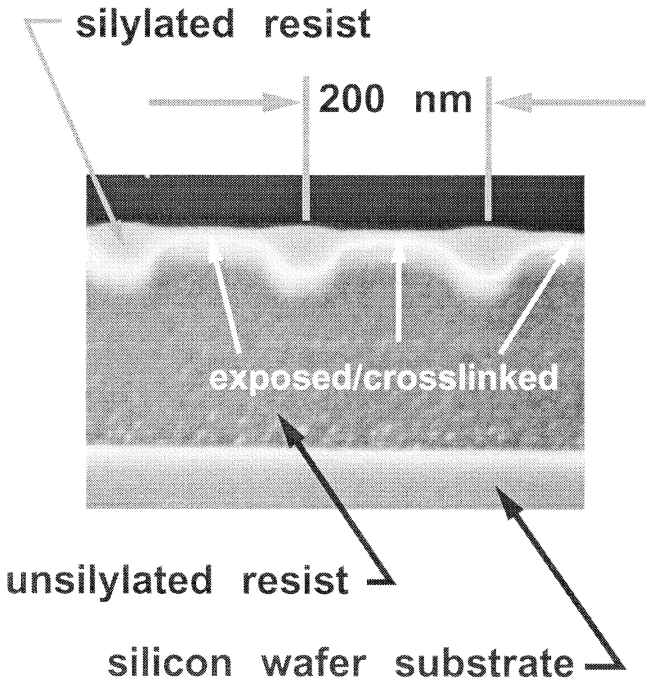

Figure 1: Cross-section plasma stain made after silylation process.

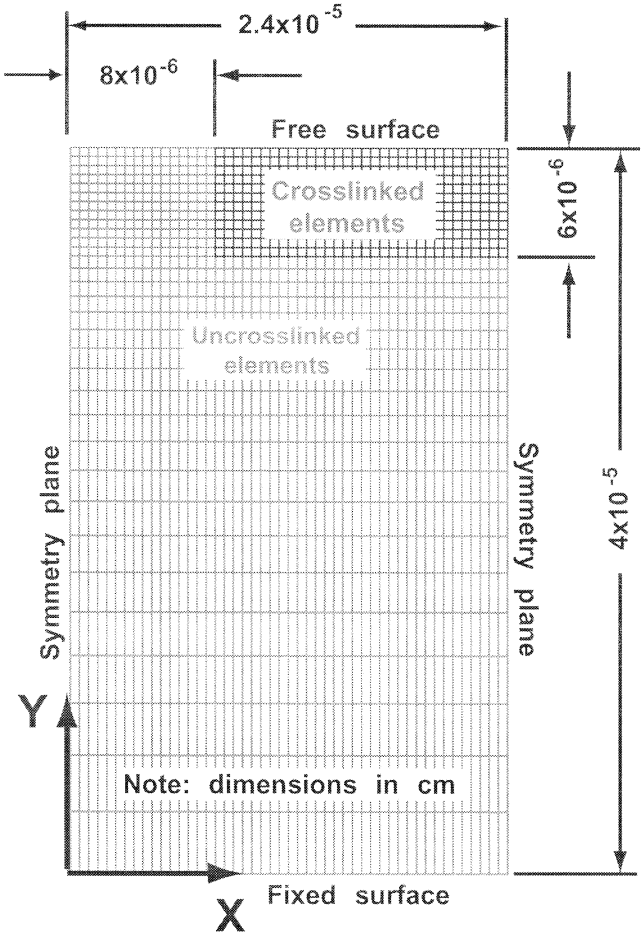

Figure 2: Finite element computational mesh.

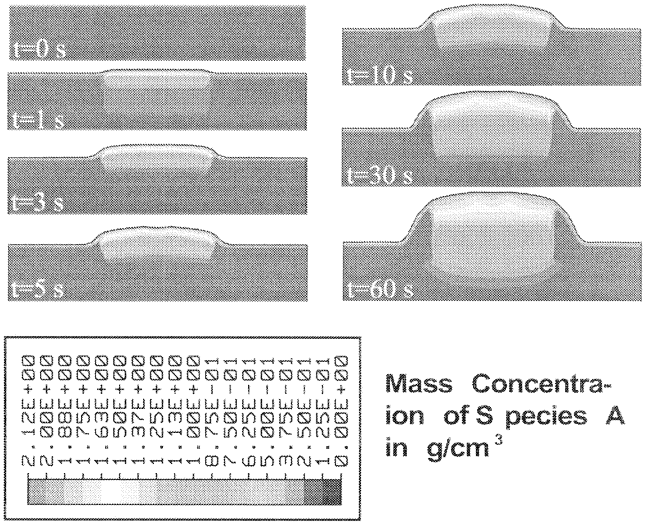

Figure 3: Transient material swelling with superimposed concentration profiles of the silylation agent.

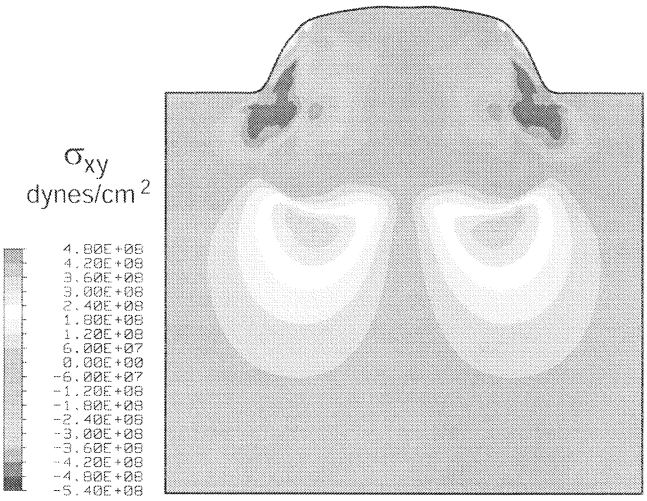

Figure 4: Residual shear stress distribution.

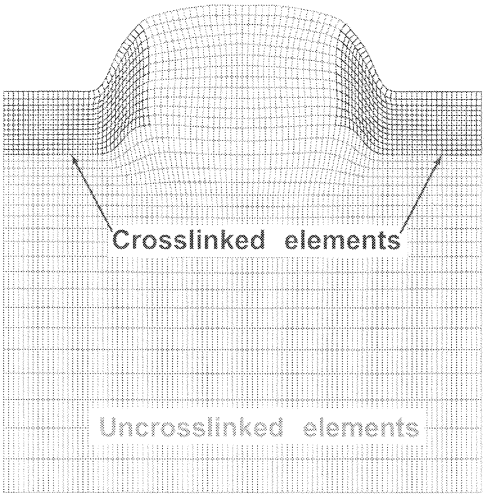

Figure 5: Final deformed mesh.